The Influence of Aerosols on the Shortwave Cloud Radiative Forcing from North Pacific Oceanic Clouds: Results from the Cloud Indirect Forcing Experiment (CIFEX)

Eric M. Wilcox
Laboratory for Atmospheres, NASA Goddard Space Flight Center

Greg Roberts and V. Ramanathan
Center for Atmospheric Sciences, Scripps Institution of Oceanography, University of California, San Diego

June 8, 2006

submitted to
Geophysical Research Letters

Corresponding author address: Eric Wilcox, NASA Goddard Space Flight Center, Code 613.2, Greenbelt MD 20771. (301) 614-6409 fax: (301) 614-6307. email: eric.m.wilcox@nasa.gov.

ABSTRACT

Aerosols over the Northeastern Pacific Ocean enhance the cloud drop number concentration and reduce the drop size for marine stratocumulus and cumulus clouds. These microphysical effects result in brighter clouds, as evidenced by a combination of aircraft and satellite observations. In-situ measurements from the Cloud Indirect Forcing Experiment (CIFEX) indicate that the mean cloud drop number concentration in low clouds over the polluted marine boundary layer is greater by 53 cm^{-3} compared to clean clouds, and the mean cloud drop effective radius is smaller by 4 μm. We link these in-situ measurements of cloud modification by aerosols, for the first time, with collocated satellite broadband radiative flux observations from the Clouds and the Earth's Radiant Energy System (CERES) to show that these microphysical effects of aerosols enhance the top-of-atmosphere cooling by -9.9 ± 4.3 W m^{-2} for overcast conditions.

1. Introduction

For oceanic scenes containing low clouds, the albedo will generally increase as the total liquid water path or geometric thickness of the cloud increases, or as the cloud fraction within the scene increases. For scenes of equivalent liquid water path, however, anthropogenic aerosols acting as additional cloud condensation nuclei (CCN) are known to increase the albedo [*Twomey*, 1977; *Coakley et al.*, 1987]. Furthermore, suppression of drizzle may impact the liquid water path and the cloud fraction [*Albrecht*, 1989; *Ackerman et al.*, 2004]. The net radiative forcing of climate attributable to these indirect aerosol effects has been determined primarily using global atmospheric models, and the magnitude remains highly uncertain [*Lohmann and Feichter*, 2005]. This study reports on the influence of aerosol variations on shortwave cloud radiative forcing over the Northeast Pacific Ocean during the April 2004 period of transpacific transport of Asian aerosols. In-situ measurements document the aerosol influence on cloud microphysics, and satellite observations determine the resulting influence on cloud radiative forcing.

Dust and anthropogenic aerosols from Asia mix with large and frequent cloud systems over the Northeast Pacific Ocean during spring. The Cloud Indirect Forcing Experiment (CIFEX) was conducted from April 1 to 21, 2004 to investigate the interactions among these aerosols and Pacific cloud systems. During 24 flights in the U. of Wyoming King Air aircraft, a full complement of microphysical measurements were made including aerosol number concentration and size distribution (Particle Cavity Aerosol Spectrometer Probe; PCASP), and cloud drop number concentration and size distribution (Forward Scattering Spectrometer Probe; FSSP). Flights were conducted from Arcata, CA (41.0 °N, 124.1 °W) to approximately 650 km offshore, alternating between 5-10 min. aerosol sampling below cloud base and 5-10 min. cloud sampling below cloud top. Aerosol concentrations during the experiment ranged from pristine

marine conditions to polluted, and two major Asian plumes containing a mix of dust and pollution were observed. Cloud systems encountered were predominantly stratocumulus and broken cumulus; some precipitating cumulus and mixed-phase clouds were also encountered. Under pristine conditions, low clouds were frequently observed to be drizzling.

Aerosols sampled during CIFEX can be sorted into six classifications based on the aerosol size distribution and back trajectories [*Roberts et al.*, 2006]. Asian air masses typically travel 3 to 7 days across the Pacific Ocean in elevated layers between 2 and 7 km. These layers are occasionally entrained into the boundary layer by vigorous vertical mixing of storm fronts. Most of the air masses in the boundary layer encountered during CIFEX were composed of cloud-processed and North American continental aerosols.

In this study we seek to document the impact of elevated concentrations of aerosol particles coincident with low clouds on the number concentration and size of cloud drops, as well as the resulting impact on shortwave cloud radiative forcing as determined by satellite albedo measurements from broadband radiometer observations. We advance a methodology that provides a quantitative measure of the enhanced shortwave cooling owing to the first aerosol indirect effect (the Twomey effect), as well as indicating the possible influence of additional aerosol impacts on cloud water amount and cloud fraction.

Measurements of cloud drop number concentration (N_d), effective radius (r_{eff}) and albedo (α) are sorted according to the number concentration of aerosol particles (N_a) in the 0.1-3.0 μm range as determined from the PCASP instrument, and evaluated as a function of cloud liquid water path (*LWP)* from the AMSR-E microwave radiometer on the Aqua satellite [*Wentz and Meissner*, 2004]. Following the methodology of *Schwartz et al.* [2002] and *Peng et al.,* [2002], cloud properties are evaluated for clouds of equivalent *LWP* to account for the strong

dependence of cloud albedo on *LWP*, which varies primarily with cloud dynamics. Furthermore, albedo and shortwave cloud radiative forcing values from CERES satellite observations are separately determined from overcast satellite footprints only, and from all satellite footprints in order to separate the contributions from the first aerosol indirect effect from differences in cloud fraction between clean and polluted samples. Observations are taken from 11 flights on 9 different days. All data have been averaged over a grid of 0.25° lat. by 0.25° lon. N_d and r_{eff} are averaged only over the cloudy samples in the grid cells, and the N_a is averaged only over the clear-air samples in the grid cells. PCASP and FSSP observations are sampled at 1 s^{-1}. *LWP* is observed in 12 km AMSR-E pixels. For analysis of overcast scenes, AMSR-E pixels are restricted to just those residing within 12 km scenes exceeding 95% cloud cover as determined by the 1 km Moderate Resolution Imaging Spectroradiometer (MODIS) cloud mask [*Ackerman et al.*, 1998].

2. Aerosol impacts on cloud microphysics

Cloud drop number concentration (N_d) and effective radius (r_{eff}) measured by the FSSP instrument are shown as a function of overcast *LWP* in fig. 1. The FSSP probe has an estimated uncertainty of 14% for r_{eff} and 25% for N_d [*Baumgardner et al.*, 1992]. Each data point is an average of observations falling within *LWP* bins of equal width along the logarithmic *LWP* scale. The vertical bars on each point are an estimate of the 95% confidence limit of the mean of all 0.25° grid cells in the *LWP* bin. The data have been further stratified into clean and polluted classes, defined as average N_a less than or greater than 50 cm^{-3}, respectively. N_a averages are restricted to samples at or below 1500 m altitude. Because the aircraft flight tracks typically alternated between level flight in the cloud layer and level flight below the cloud layer, the N_a averages largely comprise samples below cloud, and in some cases between clouds. The 50 cm^{-3}

threshold corresponds to the average aerosol concentrations (diameter > 0.1 μm) for cloud processed air-masses. Approximately one-third of all samples (including partly cloudy scenes) fall into the clean class and two-thirds in to the polluted class. The PCASP-100X probe has an estimated uncertainty of 10% for measurements of N_a. Only data where clear air N_a observations and cloudy air N_d observations coincide in the same grid cell are included. 93% of grid cells containing a cloudy air sample also contained a clear air aerosol sample, owing to the aircraft sampling pattern and the horizontal scales of the clouds.

For clouds of equivalent liquid water path, the one associated with higher aerosol concentration will exhibit a larger N_d and smaller r_{eff} if the additional aerosols have enhanced the number of CCN. This is the case for clouds observed during CIFEX. N_d is greater and r_{eff} is smaller in the clouds classified as polluted compared to the clean clouds in all but the lowest LWP bin. Averages of N_d and r_{eff} are given in table 1. r_{eff} is nearly 4 μm smaller in the polluted clouds compared to the clean clouds, and N_d is more than 50 cm^{-3} greater in the polluted clouds. The difference between clean and polluted clouds is greatest for clouds with LWP between 30 and 110 g m^{-2}, comprising more than 80% of the clouds sampled.

3. Aerosol effects on shortwave cloud radiative forcing

The CERES instrument on-board the Aqua satellite measures reflected solar radiance in the 0.3 to 5 μm spectral range [*Wielicki et al.*, 1996]. MODIS imager observations within each CERES footprint (10 km at nadir) are used to characterize the scene (including cloud fraction), and scene-specific angular distribution models are used to convert the radiances to estimates of the radiative flux [*Loeb et al.*, 2003a]. Uncertainty in the instantaneous shortwave flux at the top-of-atmosphere for cloudy-sky midlatitude scenes is estimated to be approximately 4%, and does not vary significantly with cloud optical depth or cloud fraction in liquid water clouds (*Loeb et*

al., 2003b). Shortwave cloud radiative forcing at the top of the atmosphere for diurnal mean solar insolation (C_{sm}) is determined from these observations. It is defined as the product of the diurnal mean solar insolation (S_o) and the difference between the clear-sky albedo (α_{clr}) and the cloud albedo (α):

$$C_{sm} = S_o(\alpha_{clr} - \alpha). \quad (1)$$

α_{clr} is evaluated for each satellite pass over the CIFEX region and is taken as the average albedo from cloud-free CERES ocean pixels in the region. In this first estimate of C_{sm}, α is the CERES observed albedo for overcast footprints only. Partly cloudy footprints are excluded from the analysis in order to distinguish differences in albedo owing to differences in aerosol from those owing to differences in fractional cloud cover. We report the diurnal mean C_{sm} instead of the instantaneous shortwave radiative forcing (C_s) in order to estimate the magnitude of forcing by the first aerosol indirect effect under average conditions for clouds in the CIFEX regions during April. Note, however that Aqua passes over the region at approximately 2:00 pm each day, therefore these results do not account for diurnal variations in cloud properties or variations in cloud albedo with solar zenith angle.

Albedo and C_{sm} are shown as function of LWP for the clean and polluted samples in fig. 2, where LWP averages are again limited to only overcast AMSR-E pixels. Radiative cooling by polluted clouds is greater than that of clean clouds in the 30 to 110 g m^{-2} LWP range where the increase in N_d and decrease in r_{eff} are most pronounced. Averages of C_{sm}, LWP and other quantities are summarized in table 2. The average value of C_{sm} for all overcast samples is -110.3 W m^{-2}, and the averages for clean and polluted clouds are -103.9 W m^{-2} and -113.6 W m^{-2} respectively. LWP is lower by about 4% for the overcast polluted scenes compared to the clean scenes, which is within the uncertainty of the AMSR-E observations.

To evaluate the enhancement of shortwave cloud radiative forcing owing to the greater concentration of smaller drops in the polluted clouds, we define a quantity C_{sm}^{c}:

$$C_{sm}^{c} = S_o(\alpha_{clr} - \alpha_{clean}) \tag{2}$$

where all samples in each LWP bin are assigned the average albedo for clean clouds in that bin. The resulting C_{sm}^{c} is an estimate of what the mean forcing for overcast liquid water clouds would be if N_a were always less than 50 cm^{-3}, and assuming that any difference in LWP between the clean and polluted clouds is independent of N_a. The difference, C_{sm} - C_{sm}^{c}, is then a measure of the forcing by the first aerosol indirect effect. This quantity is -9.9 ± 4.3 W m^{-2} for the low clouds observed during CIFEX. This estimate of the first indirect effect is separated from other possible indirect effects by limiting the analysis to overcast scenes and comparing clouds with equivalent LWP. Under the assumption that the slight decrease in LWP with aerosol amount are a consequence of the second indirect effect, then the difference between the mean cloud forcing and the cloud forcing averaged over the clean cloud samples only ($C_{sm}[clean]$), C_{sm} - $C_{sm}(clean)$, provides an estimate of the forcing including the LWP variations. This quantity is -6.4 W m^{-2}, which is a reduction in the cooling attributed to the Twomey effect and may reflect, at least in part, the small reduction in LWP among the polluted cases.

The quantity, -9.9 ± 4.3W m^{-2}, for net forcing owing to the first aerosol indirect effect is the average at the top of the atmosphere for overcast scenes. The overcast CERES observations account for 25% of the area observed by the satellite and aircraft. Therefore, the net forcing for mean observed conditions owing to the microphysical modification of clouds larger than the CERES footprint (at least 10 km) is -2.3 W m^{-2}.

The overcast scenes above account for 38% of cloud cover and 63% of total shortwave cloud forcing in the collocated aircraft and satellite data set. C_{sm} for all clean and polluted scenes, including partly cloudy scenes, is shown in figure 3a. The polluted scenes are generally brighter for scenes with mean LWP between 20 and 120 g m^{-2}. Note that the LWP quantities here are for mean conditions, including clean and partly cloudy AMSR-E pixels, and not representative of the overcast LWP. Therefore, in addition to the Twomey effect, differences in C_{sm} between clean and polluted clouds may be attributable to differences in cloud fraction as well. All Aqua satellite passes during April 2004 are used to compute the mean C_{sm}, as well as the clean and polluted C_{sm} for the CIFEX region, in order to account for the full variability in clouds (fig. 3b). Mean LWP and C_{sm} are averaged over 1° ocean grid cells for all Aqua passes over the region 30-50°N and 120-130°W. Samples with MODIS aerosol optical depth (*AOD*; *Remer et al.*, [2005]) less than 0.15 are classified as clean (458 samples), and samples with $AOD > 0.15$ are classified as polluted (777 samples). Shortwave cooling is enhanced for polluted scenes up to a LWP amount of about 100 g m^{-2}. Mean C_{sm} for the entire satellite data set is -29.0 W m^{-2}. The mean C_{sm} over clean and polluted samples are -17.7 and -34.2 W m^{-2}, respectively. The difference C_{sm} - $C_{sm(clean)}$ is -11.3 W m^{-2} and represents the average cooling attributable to the Twomey effect, as well as cooling attributable to differences between cloud fraction and LWP between the clean and polluted samples. Mean LWP in the polluted sample is greater by 6.5 g m^{-2} compared with the clean sample, and cloud fraction is greater by 0.15, which contributes to the enhanced cooling over that attributed to the Twomey effect. However, determining the extent to which covariations in aerosols and clouds may occur separately from second aerosol indirect effects on clouds remains uncertain and -11.3 W m^{-2} may be regarded as an upper bound on total cooling aerosol indirect effects.

4. Conclusion

The microphysical modification of low clouds by pollution in the marine boundary layer is shown to result in enhanced shortwave cooling at the top of the atmosphere in collocated satellite observations of broadband shortwave flux. Observations of low stratocumulus and cumulus clouds over the Northeast Pacific Ocean during April 2004 from the Cloud Indirect Forcing Experiment (CIFEX) indicate that N_d is greater by 53 cm^{-3} in clouds associated with aerosol number concentrations in the marine boundary layer greater than 50 cm^{-3} (for particles larger than 0.1 μm) compared with clean clouds associated with lower aerosol amounts. Cloud drop effective radius is smaller by 4 μm in polluted clouds compared with clean clouds. We show that by sorting the observed clouds by *LWP* measured with AMSR-E, these microphysical effects of aerosols can be related directly to an observed cooling at the top of the atmosphere using CERES broadband shortwave radiative flux data. Top-of-atmosphere cooling owing to the Twomey effect is -9.9 ± 4.3 W m^{-2} for overcast conditions, and -2.3 W m^{-2} for 25% cloud cover. Greater mean *LWP* and cloud fraction in the polluted clouds compared with the clean clouds results in substantial additional cooling associated with the polluted clouds, however this additional cooling cannot yet be linked directly to the microphysical modification of clouds by aerosols.

Acknowledgments. Guillaume Mauger, Odelle Hadley, John Holocek (UCSD), and Carl Schmidt (NCAR) contributed to the planning and execution of CIFEX. We are also grateful for efforts of the U. of Wyoming King Air crew. CERES data were obtained from the NASA Langley Research Center DAAC. CIFEX was funded by the National Science Foundation. The lead author was supported by a fellowship from the NOAA Postdoctoral Program in Climate and Global Change administered by the University Corporation for Atmospheric Research.

References

Ackerman, A. S., M. P. Kirkpatrick, D. E, Stevens, and O. B. Toon, 2004: The impact of humidity above stratiform clouds on indirect aerosol climate forcing. *Nature*, **432**, 1014-1017.

Ackerman, S. A., K. I. Strabala, W. P. Menzel, R. A. Frey, C. C. Moeller, and L. E. Gumley, 1998: Discriminating clear-sky from clouds with MODIS. *J. Geophys. Res.*, **103**, 32 141-32 158.

Albrecht, B. A., Aerosols, cloud microphysics, and fractional cloudiness, *Science*, **245**, 1227-1230, 1989.

Baumgardner D., J. E. Dye, B. W. Gandrud, R. G. Knollenberg, 1992: Interpretation of Measurements Made by the Forward Scattering Spectrometer Probe (FSSP-300) During the Airborne Arctic Stratospheric Expedition, *J. Geophys. Res.*, **97**, 8035-8046.

Brenguier, J.-L., H. Pawlowska, and L. Schüller, 2003: Cloud microphysical and radiative properties for parameterization and satellite monitoring of the indirect effect of aerosol on climate, *J. Geophys. Res.*, **108**, 8632, doi:10:1029/2002JD002682.

Coakley, J. A. Jr., R. L. Bernstein, and P. A. Durkee, 1987: Effect of Ship-Stack Effluents on Cloud Reflectivity, *Science*, **237**, 1020-102.

Loeb, N. G., N. Manalo-Smith, S. Kato, W. F. Miller, S. K. Gupta, et al., 2003a: Angular distribution models for top-of-atmosphere radiative flux estimation from the Clouds and the Earth's Radiant Energy System instrument on the Tropical Rainfall Measuring Mission satellite. Part I: Methodology, *J. Appl. Meteor.*, **42**, 240-265.

Loeb, N. G., N. Manalo-Smith, S. Kato, W. F. Miller, S. K. Gupta, et al., 2003b: Angular distribution models for top-of-atmosphere radiative flux estimation from the Clouds and the Earth's Radiant Energy System instrument on the Tropical Rainfall Measuring Mission satellite. Part II: Validation, *J. Appl. Meteor.*, **42**, 1748-1768.

Lohmann, U. and J. Feichter, 2005: Global aerosol indirect effects: a review, *Atmos. Chem. Phys.*, **5**, 715-737.

Peng, Y., U. Lohmann, R. Leaitch, C. Banic, and M. Couture, 2002: The cloud albedo-cloud droplet effective radius relationship for clean and polluted clouds from RACE and FIRE.ACE, *J. Geophys. Res.*, **107**, doi:10.1029/2000JD000281.

Remer, L. A., Kaufman, Y, J., D. Tanre, S. Mattoo, D. A. Chu, et al., 2005: The MODIS aerosol algorithm, products and validation. *J. Atmos. Sci.*, **62**, 947-973.

Roberts, G., G. Mauger, O. Lariviere, and V. Ramanathan, 2005: Aerosols over the Eastern Pacific Ocean and their relationships to cloud condensation nuclei, *J. Geophys. Res., in press.*

Schwartz, S. E., Harshvardhan, and C. M. Benkovitz, 2002: Influence of anthropogenic aerosol on cloud optical depth and albedo shown by satellite measurements and chemical transport modeling, *Proc. Natl. Acad. Sci.*, **99**, 1784-1789.

Twomey, S., 1977: The influence of pollution on the shortwave albedo of clouds, *J. Atmos. Sci.*, **34**, 1149-1152.

Wentz, F., and T. Meissner. 2004, updated daily: *AMSR-E/Aqua L2B Global Swath Ocean Products derived from Wentz Algorithm V001*, March to June 2004. Boulder, CO, USA: National Snow and Ice Data Center. Digital media.

Wielicki, B. A., B. R. Barkstrom, E. F. Harrison, R. B. Lee III, G. L. Smith, and J. E. Cooper, 1996: Clouds and the Earth's Radiant Energy System (CERES): An Earth Observing System Experiment, *Bull. Amer. Meteor. Soc.*, **77**, 853-868.

Table 1. Mean microphysical properties and cloud cover by aerosol concentration classification.

	Aerosol number conc. (N_a cm^{-3}; 0.1-3μm diameter)	Cloud drop number conc. (N_d cm^{-3})	Cloud drop effective radius (r_{eff} μm)
clean	33	21	13.7
polluted	124	74	9.7
average	90	55	11.1

Table 2. Cloud properties and shortwave cloud radiative forcing for average, clean, and polluted overcast scenes.

	ave.	clean	polluted
num. of samples		18	35
C_{sm} (± 4 W m^{-2})	-110.3	-103.9	-113.6
N_a (± 9 cm^{-3})	89.9	34.0	118.6
LWP (± 17 g m^{-2})	159.4	162.4	157.9
C_{sm}^{c} (± 4 W m^{-2})	-100.4		
$C_{sm} - C_{sm}^{c}$ (± 4 W m^{-2})**	-9.9		
$C_{sm} - C_{sm}(clean)$ (± 4 W m^{-2})++	-6.4		

Uncertainties are published estimates of RMS error.
** forcing by 1st indirect effect.
++ forcing by combined 1st and 2nd indirect effects.

Figure captions

Figure 1: (a) Cloud drop number concentration (N_d), and (b) cloud drop effective radius (r_{eff}) from aircraft FSSP measurements. Both are shown as a function of cloud liquid water path (LWP) for clean and polluted clouds. Number of 0.25° grid cells is 113, comprising 17,748 1 s FSSP samples.

Figure 2: (a) Albedo (α), and (b) diurnal mean shortwave cloud radiative forcing (C_{sm}) for overcast CERES footprints. Both are shown as a function of cloud LWP for clean and polluted clouds. Number of 0.25° grid cells is 53.

Figure 3: Diurnal mean shortwave cloud radiative forcing (C_{sm}) for all 0.25° grid cells including overcast and partly cloudy scenes. (a) Collocated aircraft and Aqua satellite data. Clean and polluted determined from in-situ N_a. Number of 0.25° grid cells is 198. (b) All April 2004 Aqua overpasses. Polluted is MODIS aerosol optical depth greater than 0.15. Number of 1° grid cells is 1235.

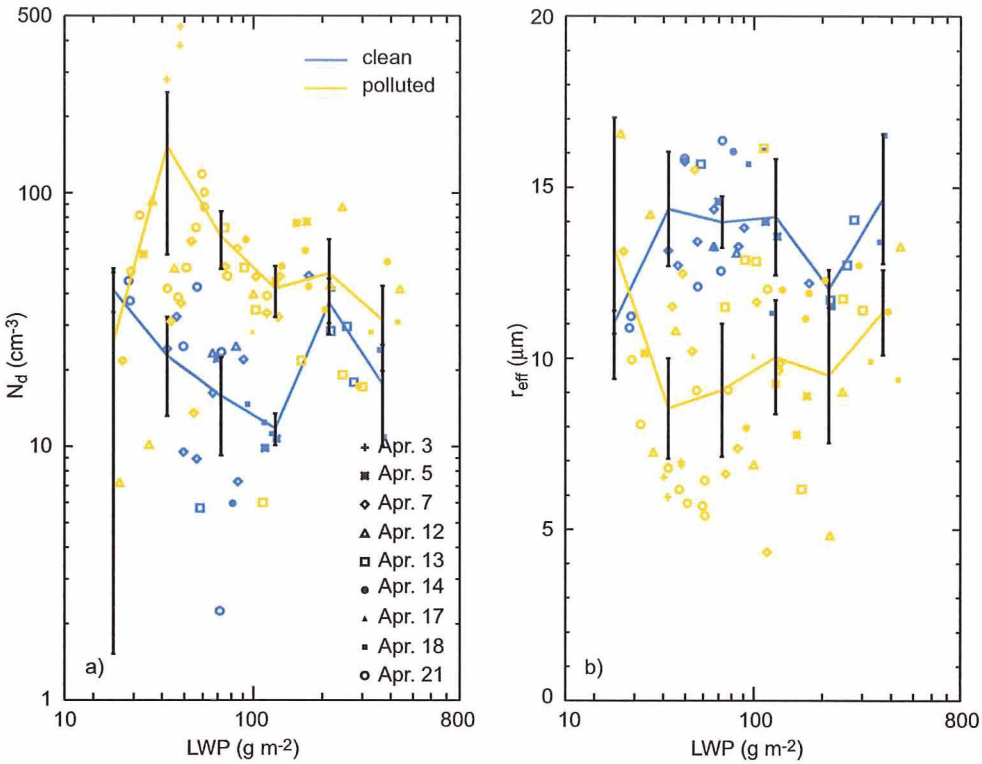
500
100
10
1
N_d (cm^{-3})
clean
polluted
Apr. 3
Apr. 5
Apr. 7
Apr. 12
Apr. 13
Apr. 14
Apr. 17
Apr. 18
Apr. 21
a)
10
100
800
LWP (g m^{-2})
20
15
10
5
0
r_{eff} (μm)
b)
10
100
800
LWP (g m^{-2})

Figure 1

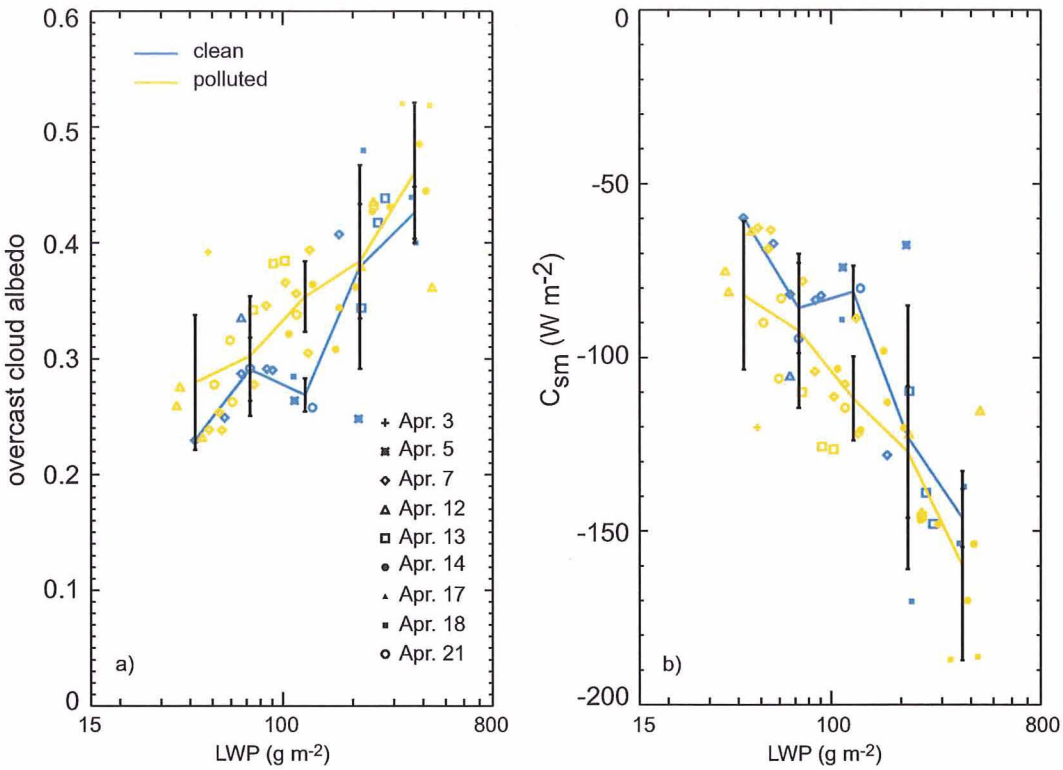
clean
polluted
Apr. 3
Apr. 5
Apr. 7
Apr. 12
Apr. 13
Apr. 14
Apr. 17
Apr. 18
Apr. 21
a)
b)
overcast cloud albedo
C_{sm} (W m^{-2})
LWP (g m^{-2})
LWP (g m^{-2})
0.6
0.5
0.4
0.3
0.2
0.1
0
-50
-100
-150
-200
15
100
800

Figure 2

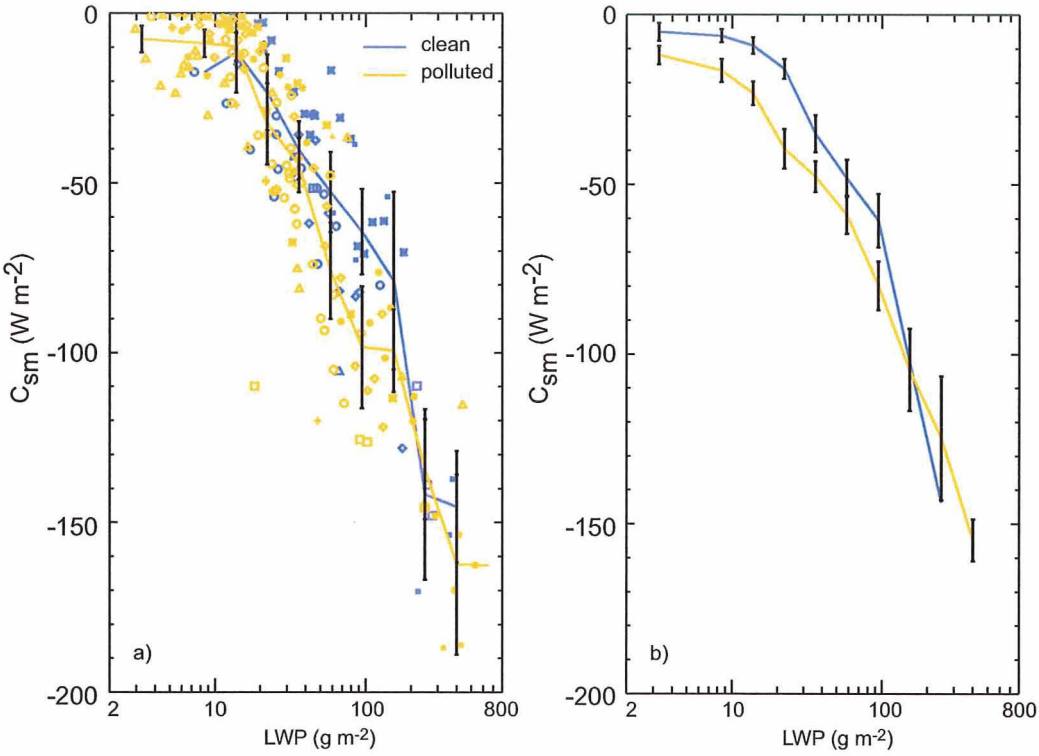

Figure 3